

Optical properties of layered transition-metal iodides

I. Pollini

*Dipartimento di Fisica, Università di Milano and Gruppo Nazionale di Struttura della Materia
del Consiglio Nazionale delle Ricerche, Via Celoria 16, I-20133 Milano, Italy
and Laboratoire d'Utilisation du Rayonnement Electromagnétique, Université de Paris—Sud, F-91405 Orsay, France*

J. Thomas

*Laboratoire de Spectroscopie, Université de Rennes I, F-35010 Rennes, France
and Laboratoire d'Utilisation du Rayonnement Electromagnétique, Université de Paris—Sud, F-91405 Orsay, France*

A. Lenselink

*Laboratory of Inorganic Chemistry, State University of Groningen, 9747-AG Groningen, The Netherlands
and Laboratoire d'Utilisation du Rayonnement Electromagnétique, Université de Paris—Sud, F-91405 Orsay, France*

(Received 19 March 1984)

Low-temperature reflectance data from layered single crystals of FeI_2 , CoI_2 , and NiI_2 have been obtained in the ultraviolet region of the spectrum up to 31 eV with synchrotron radiation, and the high-frequency dielectric tensor elements $\epsilon_{xx}^T(E)$ have been deduced by Kramers-Kronig analysis. The spectra can be described in terms of single-particle (charge transfer, direct interband transitions, and excitons) and collective excitations (valence-electron plasma oscillations). The presence of collective effects is indicated by a plasma resonance which corresponds roughly to an electron density of 12 per molecule. Following recent calculations for the band structures of transition-metal chlorides and NiBr_2 and basing our analysis on the experimental data, we found it possible to interpret the low-lying transitions satisfactorily. In particular, the direct energy gap is assigned to $\Gamma_3^- \rightarrow \Gamma_1^+$ transitions in FeI_2 (6 eV), CoI_2 (6.15 eV), and NiI_2 (6.26 eV). Furthermore, the interpretation of the satellite exciton located at the low-energy side of the Γ doublet in iodide compounds is attempted in terms of the Onodera-Toyozawa theory by considering the exchange interaction of the triplet-exciton electron in the itinerant $4s$ states with localized magnetic moment of the metal $3d$ electrons.

I. INTRODUCTION

In previous papers¹⁻³ we have discussed the vacuum ultraviolet reflectance spectra of ionic layered nickel dihalides and have shown how the spectral structures can be divided into charge transfer bands, exciton peaks, and direct interband structures. We have also noticed that the prominent low-energy features in the spectrum of crystalline NiI_2 are very similar to those observed in the optical spectra of NiCl_2 and NiBr_2 . With regard to the appearance of a weaker peak at the low-energy side of the first doublet exciton Γ in NiBr_2 and NiI_2 , we have suggested that this satellite exciton could probably be assigned to a triplet exciton activated by strong exciton-phonon interaction, as discussed by Onodera-Toyozawa (OT) long ago.⁴ In the present work we present new experimental results on NiI_2 , CoI_2 (α form), and FeI_2 in order to extend our studies to the excitonic and interband scattering region of transition-metal iodides (TMI), which have not been greatly studied so far. In fact scarce optical measurements have been made on only a few layer materials, viz., those where it has been possible to get suitably large stable crystals or good quality films. Apart from the room-temperature absorption measurements on CoI_2 and NiI_2 obtained by Fesefeldt⁵ in a limited range (2–6 eV), the only knowledge of optical spectra we have is on the

liquid-nitrogen temperature absorption spectra on evaporated films of MnI_2 and FeI_2 up to 6–7 eV.⁶

FeI_2 , CoI_2 , and NiI_2 are ionic insulators which crystallize in layerlike structures. NiI_2 has a crystal structure of the CdCl_2 type,⁷ space group D_{3d}^5 ; CoI_2 and FeI_2 crystallize in the $\text{Cd}(\text{OH})_2$ -type structure,⁷ space group D_{3d}^3 , though also for CoI_2 the CdCl_2 -type structure has been claimed.⁸ These TMI usually crystallize as platelets perpendicular to the c axis. The metal ions in NiI_2 , CoI_2 , and FeI_2 have an octahedral coordination of iodine ions. The metal ions have localized magnetic moments due to the partly occupied d shell with $S=1$ (NiI_2 , $3d^8$), $S=\frac{3}{2}$ (CoI_2 , $3d^7$), and $S=2$ (FeI_2 , $3d^6$). At low temperature the magnetic moments order antiferromagnetically; the magnetic ordering temperatures of NiI_2 , CoI_2 , and FeI_2 are 75 K,⁹ 3 K (Ref. 10) to 12 K (Ref. 9), and 10 K,¹¹ respectively.

In Sec. II the sample preparation and the experimental techniques are described. In Sec. III the optical spectra of TMI and the plots of the complex dielectric function $\hat{\epsilon}=\epsilon_1+i\epsilon_2$ and optical energy-loss function $-\text{Im}(1/\hat{\epsilon})$ are presented. Finally, in Sec. IV, consideration of MgX_2 (Refs. 12–14) and NiX_2 (Ref. 15) ($X=\text{Cl},\text{Br}$) calculated electronic structures has allowed us to describe satisfactorily the low-lying single-electron transitions.

II. EXPERIMENTAL PROCEDURES

A. Sample preparation

NiI_2 , CoI_2 , and FeI_2 were prepared starting from the elements using metal power (Koch-Light, purity over 99.99%) and two times sublimed iodine (Merck, purity over 99.5%). Quartz ampoules were kept in a furnace ($\sim 150^\circ\text{C}$) for several days to remove any water. After filling with metal powder and iodine the ampoules were evacuated, sealed, and placed in a tube furnace with the empty side of the ampoule just outside the furnace in order to prevent too high an iodine pressure. In the case of NiI_2 the temperature was slowly raised to about 600°C – 700°C , while for CoI_2 and FeI_2 the temperature was kept at about 500°C . Since these last two compounds melt [CoI_2 (Ref. 16)] or decompose [FeI_2 (Ref. 17)] just above 500°C it is crucial to monitor the furnace temperature precisely. The reactions were completed within one or two weeks. After purification via sublimation single crystals were prepared both by Bridgman technique and chemical transport method. The preparation of single crystals of NiI_2 presented some problems, since its growth in a Bridgman oven is hampered by decomposition into metallic nickel and an iodine-rich phase at 740°C – 760°C .^{16–18} Alternatively using the chemical transport method, thin platelets of all three iodides could be obtained. Iodide compounds prepared as described above were sealed in a quartz ampoule with little excess of free iodine and placed in the tube furnace. Along the ampoule was a temperature gradient of 750°C – 650°C (NiI_2), 520°C – 400°C (CoI_2), 520°C – 470°C (FeI_2), resulting in a slow transport of the material from one side to the other. After some weeks, thin, black, shiny crystals of NiI_2 and CoI_2 and red crystals of FeI_2 were collected from the growth tube.

B. Experimental method

Ultraviolet radiation from the electron storage ring of ORSAY (Laboratoire d'Utilisation du Rayonnement Electromagnetique, Universite de Paris-Sud) was used as the continuum light source. The monochromator spectral bandwidth was better than 6 Å. Strong interband transitions are practically exhausted in ionic insulators below 30 eV, which is the practical limit of our measurements. In all our experiments we investigated the optical reflectivity of crystal planes perpendicular to the c axis, with the electric vector of the light approximately perpendicular to the c axis.

The incident and reflected light was detected by a sodium salicylate-coated photomultiplier (Hamamatsu, R-268) in the whole energy region. Crystals grown by both methods were employed in the reflectance measurements. No effects due to the preparation method have been noticed. Since all crystals are rather hygroscopic, all handling had to be performed in a glove box flowed with dry nitrogen gas. The measurements were performed at 300 and 30 K in a vacuum of about 10^{-9} – 10^{-10} Torr.

III. EXPERIMENTAL RESULTS AND CONSIDERATIONS

Figures 1–3 show the survey reflectance spectra of single crystals of FeI_2 , CoI_2 , and NiI_2 at 300 K. These

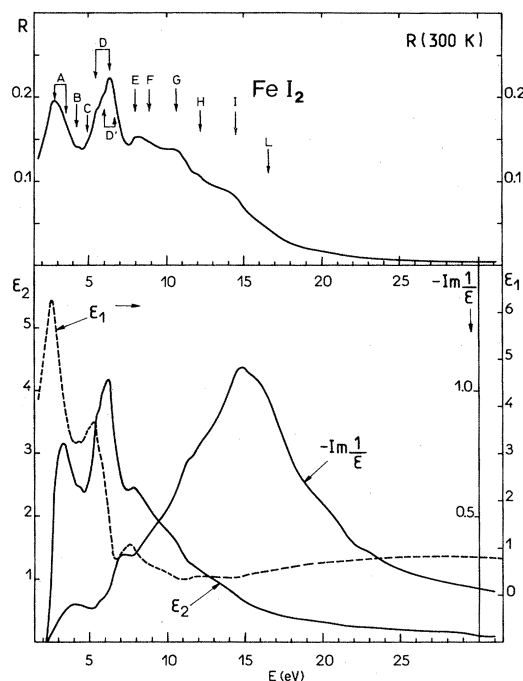


FIG. 1. Spectral dependence of the reflection R , the real and imaginary parts of the dielectric function ϵ_1 and ϵ_2 , and the energy-loss function $-\text{Im}(1/\hat{\epsilon})$ for FeI_2 at room temperature.

curves show typical results for these insulators. Two spectral regions can be distinguished. The first region extending to about 10–12 eV is characterized by sharp structure associated with charge transfer transitions to metal d states and interband transitions to metal s states.

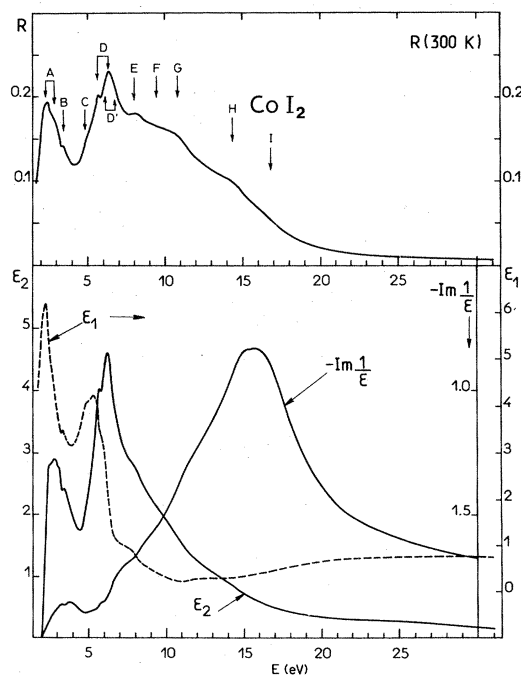


FIG. 2. Spectral dependence of the reflection R , the real and imaginary parts of the dielectric function ϵ_1 and ϵ_2 , and the energy-loss function $-\text{Im}(1/\hat{\epsilon})$ for CoI_2 at room temperature.

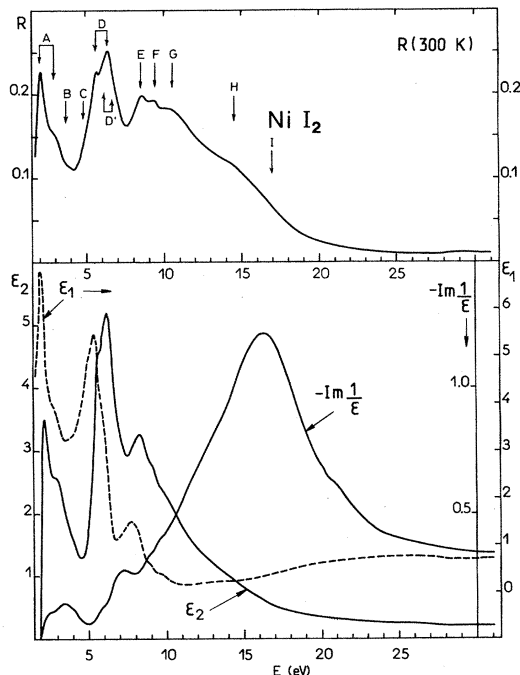


FIG. 3. Spectral dependence of the reflection R , the real and imaginary parts of the dielectric function ϵ_1 and ϵ_2 , and the energy-loss function $-\text{Im}(1/\hat{\epsilon})$ for NiI_2 at room temperature.

The second region, which extends to about 25 eV, is marked by a strong decrease of the reflectance which becomes less than 5% beyond 18–20 eV. The spectral dependence of the complex dielectric function $\hat{\epsilon}(E) = \epsilon_1 + i\epsilon_2$ and the imaginary part of $1/\hat{\epsilon}(E)$ for TMI are also presented in Figs. 1–3. The energy-loss function, $-\text{Im}[1/\hat{\epsilon}(E)]$, is of considerable interest, since it contains detailed information on the energy state structure of the valence electrons in the crystals. It is known that, when the single-electron excitations are described by screened quasielectrons, there appears in a solid a new excitation mode consisting of quantized high-frequency collective oscillations of the valence electrons (plasmons), because of the long-range component of the Coulomb interaction.¹⁹ The plasma energy in semiconductors or insulators is rather higher than the energy separation between valence and conduction bands, usually something less than 6 or 10 eV, and varies from about 13 to 30 eV, corresponding to a valence-electron density of the order of 10^{23} – 10^{24} cm^{-3} .²⁰ As a result, plasma excitations are only observed by supplying energy to the electron system from the outside, typically when one fires fast electrons through the solid.²¹ The optical effect which comes closest to the stopping power is the nonrelativistic Compton effect of about 10-keV photons²² and, besides all these effects are closely related to the transverse properties of solids, such as the far-ultraviolet optical properties or the x-ray absorption and emission. In fact, in the limit of long wavelengths the response of electrons to either transverse (photons) or longitudinal (electrons) disturbances may be described in terms of the same quantity. In particular, the random phase approximation shows the equal-

ity of the transverse ϵ_{\perp} and longitudinal ϵ_{\parallel} dielectric constants in a straightforward manner.^{23–25} Further, if one works with anisotropic single crystals, as TMI, one must take care to compare dielectric constants for the same direction of polarization [in our case $\epsilon_{xx}^T(E) = \epsilon_{yy}^T(E)$].

We notice that the function $-\text{Im}(1/\hat{\epsilon})$ for TMI, which describes the energy loss of fast electrons traversing the material, presents some overlap between single-electron and plasma excitations and strong maxima around 15–18 eV are observed. Maxima can be thus associated with the existence of plasma oscillations. In this energy region the valence electrons of TMI are essentially unbound and are able to perform collective oscillations. From Figs. 1–3 we see that the function $-\text{Im}[1/\hat{\epsilon}(E)]$ exhibits maxima around 15, 15.8, and 16.5 eV for FeI_2 , CoI_2 , and NiI_2 , respectively. This oscillation energy can be calculated by means of the Horie's formula, which takes into account the number of valence-band electrons participating in the collective process and the interband energy gap E_g of the material.²⁶ By considering the values of E_g we obtained for FeI_2 , CoI_2 , and NiI_2 the theoretical values of 14.4, 14.8, and 15.0 eV, respectively.

Figure 4 shows detailed reflectance spectra of TMI at 300 and 30 K. We notice that the spectra of CoI_2 and FeI_2 are very similar to that of NiI_2 ,^{2,3} as expected on account of the similar ionic constitution. The two peaks A are assigned to $p \rightarrow d$ excitons associated with the charge transfer transition $5p^6 3d^{n-1} \rightarrow 5p^5 3d^n$ ($n=7,8,9$ from Fe to Ni) which produce the following broad and weak structure B . The strong peaks D are assigned to $p \rightarrow s$ excitons connected with the lowest interband edge, on account of their temperature behavior (see Figs. 5 and 6) and their

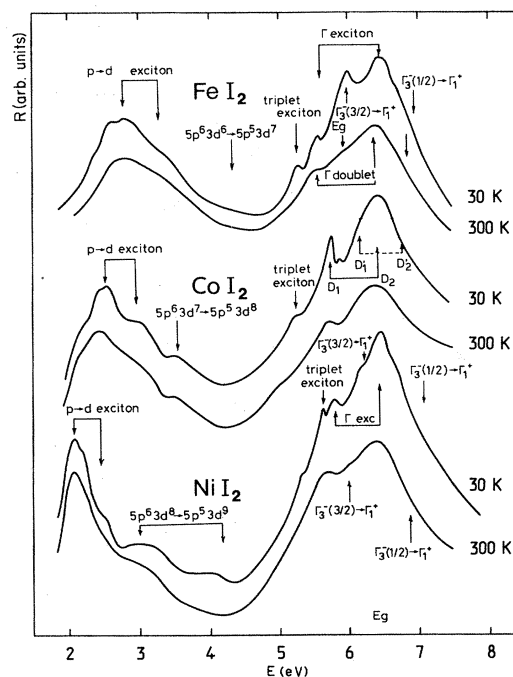


FIG. 4. Details of the exciton charge transfer ($p \rightarrow d$), exciton and band-to-band ($p \rightarrow s$) transitions for FeI_2 , CoI_2 , and NiI_2 crystals at 300 and 30 K.

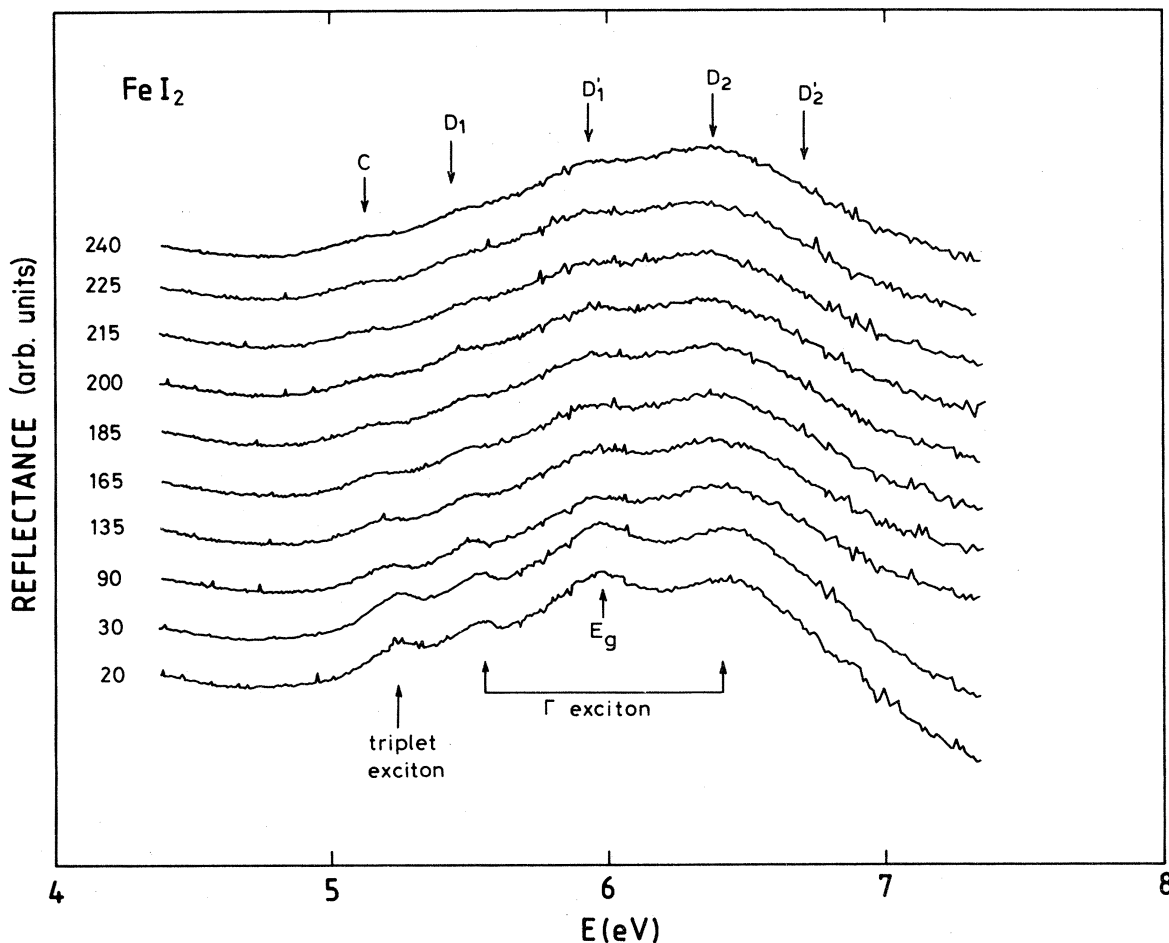


FIG. 5. Reflectance spectra of FeI_2 taken at fixed temperatures in the excitonic and interband regions.

spin-orbit splitting, whose order of magnitude for TMI is around 0.75–0.85 eV. By considering the energy position of the $p \rightarrow s$ excitons, we may suggest the values of the forbidden energy gap E_g for TMI; $E_g = 6.0$ eV for FeI_2 , 6.15 eV for CoI_2 , and 6.25 eV for NiI_2 . It is not so easy to fix the exact values of E_g since the reflectance spectra get complicated at low temperatures for the intervention of magnetic effects. Of course this in turn complicates the task of estimating the plasma energies by using the values of E_g which should be then considered only tentative at this stage of the research.

In Fig. 7 we have plotted the dielectric function $\epsilon_{\text{eff}}(E)$ and $N_{\text{eff}}(E)$ obtained by means of the sum rules. It is immediately seen that beyond about 12–13 eV the curves of ϵ_{eff} for TMI saturate at values of 3.8, ~ 4 , and 4.4 for FeI_2 , CoI_2 , and NiI_2 , respectively. A general discussion of the experimental values of the dielectric tensor elements $\epsilon_{xx}^T(0, E) = \epsilon_{yy}^T(0, E)$ for transition metal halides, measured by means of optical reflectance for light traveling parallel to the c axis, and their comparison with the extended-shell-model predictions for the whole series has been made in a previous work,²⁷ which we refer to for more information.

Additional information of considerable value in the experimental study of band structures can be obtained from

the curves of $\epsilon_2(E)$ and the oscillator integral function $N_{\text{eff}}(E)$. In fact most band-structure calculations are able to predict quite accurately the dispersion curve $E(\vec{k})$ but are less certain in predicting the energy distances between bands due to lack of good self-consistency. An experimental evaluation of $\epsilon_2(E)$ and $N_{\text{eff}}(E)$ can therefore be used to verify the actual degree of overlap between the contributions of different band groups. Coming to TMI, we notice a great similarity between the curves of $R(E)$ or $\epsilon_2(E)$ for the different iodides. In fact, except for minor energy shifts, the spectra of FeI_2 , CoI_2 , and NiI_2 reported in Figs. 1–3 may nearly be superimposed. Three prominent structures can be identified in $R(E)$ or $\epsilon_2(E)$ at an energy of about 2–3 eV (peaks A and B), 6–7 eV (D and D'), 8–10 eV (E, F, G), and 14–15 eV (H). One expects the valence and conduction bands in the three transition-metal halides FeI_2 , CoI_2 , and NiI_2 to be essentially the same; the differences in the spectra are mainly due to a different occupation of the d levels. From the plots of $N_{\text{eff}}(E)$ one sees that the first peaks in $\epsilon_2(E)$ (peaks A and B of the reflectance spectra in Figs. 1–3) correspond to about 2, 3, and 4 electrons excited in NiI_2 , CoI_2 , and FeI_2 ; the second peaks (peak D and D') to 5–6 electrons excited per molecule and finally the remaining structure to 6 electrons per formula unit [peaks E , F , and G of $R(E)$].

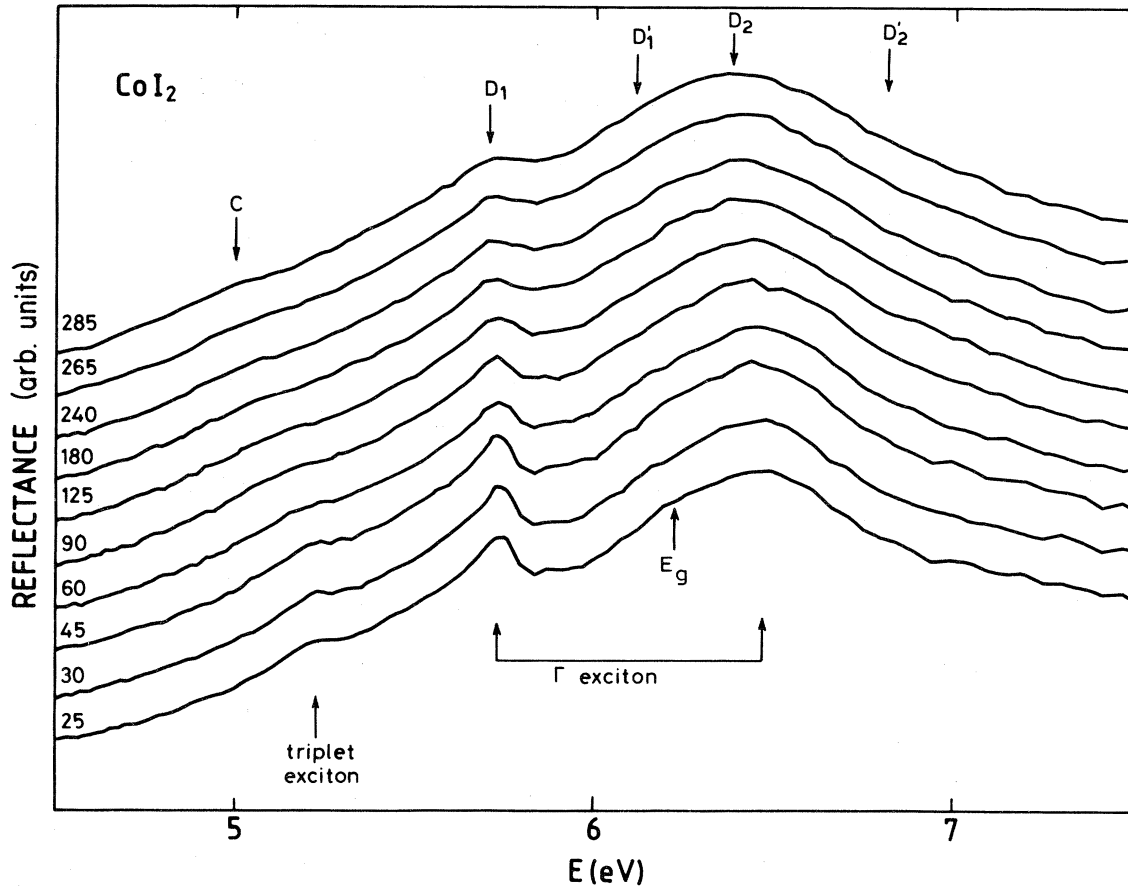


FIG. 6. Reflectance spectra of CoI_2 taken at fixed temperatures in the excitonic and interband regions.

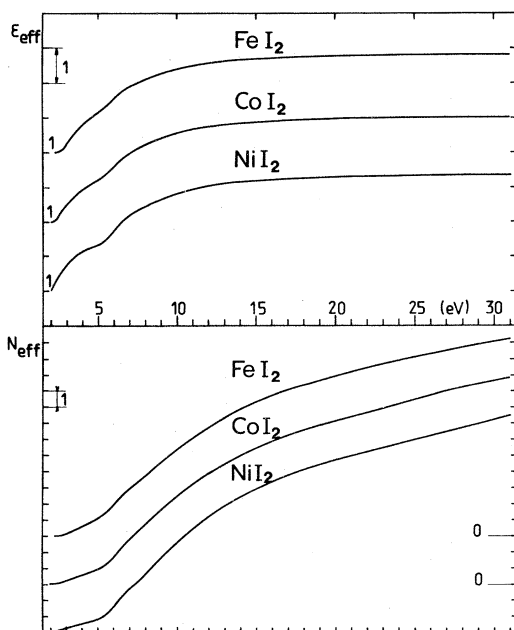


FIG. 7. Effective dielectric constant $\epsilon_{\text{eff}}(E)$, and effective number of electrons, $N_{\text{eff}}(E)$, for FeI_2 , CoI_2 , and NiI_2 .

The fact that $N_{\text{eff}}(E)$ shows “partial” saturation at values below the number of valence electrons indicates that a group of strong transitions from the valence band to upper d -level groups or to the conduction band has been exhausted. Thus we regard peaks A and B as representative of charge transfer transitions filling the quasilocalized d states; peaks D and D' are attributed to excitonic and interband transitions to the lowest conduction band (primarily of metal s type); and peaks E through H to critical point transitions to upper conduction bands until the region of plasma oscillations is reached.

As already pointed out, the “experimentally” observed plasma excitations lie in an energy range where the oscillator strengths corresponding to both $I^- p$ and $M^{2+} 4s$ bands are relatively weak; however, some overlap between electron and plasmon interactions is observable (Figs. 1 and 3). We may also remark that the energy-loss line is not narrow (as it happens in many metals), but rather broad presenting an energy peak somewhat displaced from the free value electron plasma energy, for which we have calculated the values of 13.1, 13.5, and 13.6 eV for FeI_2 , CoI_2 , and NiI_2 , respectively. The bandwidth is an indication that the collective excitation has a short lifetime, since there are quite a number of single-particle transi-

tions in its immediate vicinity.²⁸ in Figs. 1–3 we see that the overlap region extends between 10 and 15 eV. This will cause the damping of the plasma waves in the crystal, mainly because of the linear electron-plasmon interaction.^{29,30} This is not in contrast with the fact that one should expect in principle that, whenever there is a shift in the plasmon energy from the free electron value, there should be correspondingly broadening of the observed energy loss peak. Clearly peaks in the energy loss function can be associated either with a plasma oscillation or with interband transitions. Of course, the two physical phenomena can be distinguished rather unambiguously if the dielectric constants in the vicinity of such peaks are known. Certainly single-electron band-band transitions take place in our spectra; for instance, the energy losses observed in the lowest energy region (2–5 eV) may be easily associated with a iodine *p*-electron transfer to the neighboring cation *d* shell.

IV. DISCUSSION

In order to interpret the ultraviolet spectra of TMI, it seems useful at this point to recall the main results of band-structure calculations for TM chlorides and NiBr₂ (same crystal structure as NiI₂) (Ref. 7) and the state of the present understanding of the valence and conduction bands. The upper valence-band structure has been shown to arise from the highest filled Cl 3*p* or Br 4*p* states of the halogen ion. The low-lying bands associated with Cl 3*s* or

Br 4*s* atomic levels are not reported in Fig. 8 since they lie between 18 and 16 eV, respectively, below the top of the valence band. The uppermost valence bands of NiCl₂ and NiBr₂ (Fig. 8) show maxima at Γ (Γ_3^- symmetry) and are relatively flat between Γ and Z, i.e., they depend very little on the wave vector \vec{k} along the symmetry line Λ . On the other hand, there appears to be a rather strong dependence of \vec{k} in other directions and for the lower branches of the valence band for both crystals. The complex structure of the conduction bands is also indicated in Fig. 8. The lowest conduction band is mainly determined by the positive ions in the lattice being primarily of Ni 4*s* character and has an absolute minimum at Γ (Γ_1^+ symmetry). Above this lowest branch other conduction states are found at $Z_2^-, F_1^+, L_2^-, F_2^-, \Gamma_2^-$. The band structure of NiX₂ (X=Cl,Br) displays, in addition, five more narrow bands originating from 3*d* states, which lie in the “forbidden” gap between halogen *p* levels and metal *s* states. However, the properties of the *d* electrons are not described adequately with a one-electron band theory as developed by Antoci and Mihich, due to the large correlations between the *d* electrons. In fact, a strict application of the band picture of Antoci and Mihich would lead to a partly occupied *d* band, with 6, 7, and 8 *d* electrons for FeI₂, CoI₂, and NiI₂. For CoI₂ and NiI₂ the Fermi level would then lie in the upper *d* bands, and this would lead to metallic conduction. This is certainly not the case, for all three compounds are good insulators, indicating that

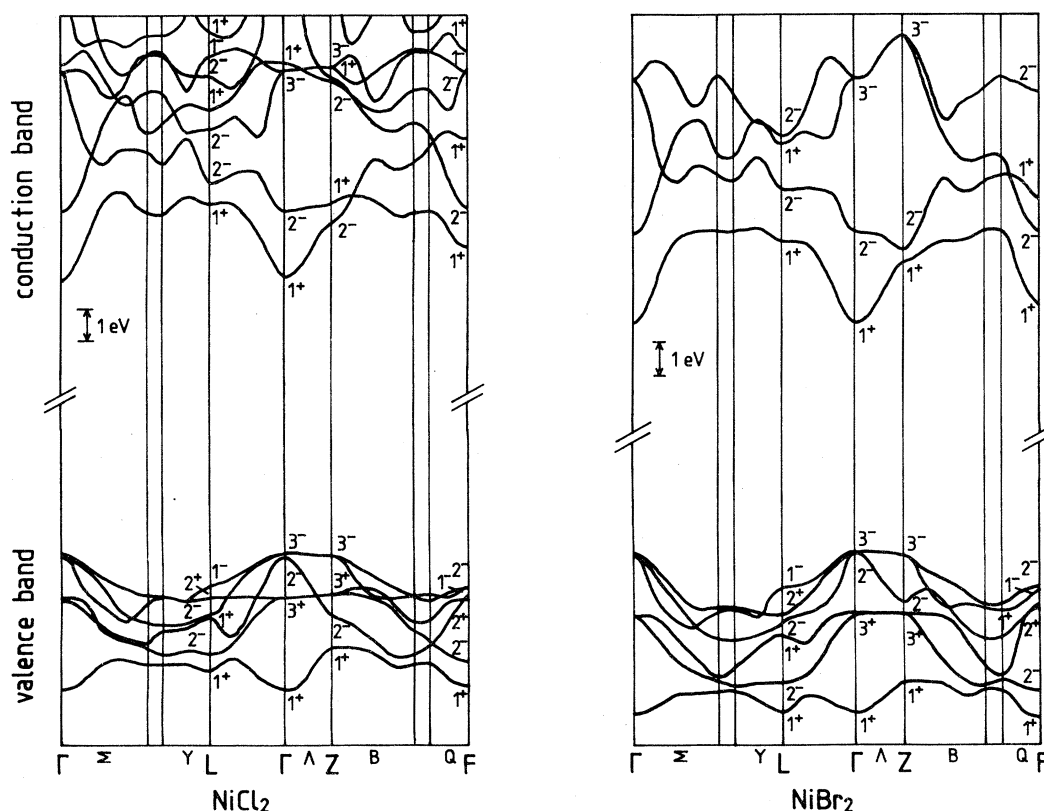


FIG. 8. Band structure of NiCl₂ and NiBr₂ following Antoci and Mihich (Ref. 15). For sake of clarity metal *d* bands and higher conduction bands have been left out.

the d electrons cannot be described by band theory. The value of the gap and the location of the two narrow (quasimolecular) d bands is to be determined experimentally. Looking for more theoretical support, we found that the only family of materials which present some similarities with TMI on the ground of structural and symmetry considerations are the layered transition-metal chalcogenides (TMC) MX_2 with $M=\text{Ti,Zr,Hf}$ and $X=\text{S,Se,Te}$, which present octahedral coordination of the cation. It is seen, for example, that the basis features of the band model^{31,32} for octahedral structure, e.g., ZrS_2 , ZrSe_2 , and HfS_2 , are similar to those of transition-metal halides (TMH). The difference is due to the dispersion of the d states which form d bands about 1.8–2.2 eV wide in contrast with TMH where the d states are localized. This fundamental difference in the structure of d states, due to the different degree of covalency of TMC, and also the different occupancy of the d levels determines the different electrical properties of these semiconducting materials. The degree of covalency may be judged from consideration of the figures of the fractional ionic band character f_i which, according to Gamble,³³ for the reported TMC varies from 0.30 to 0.10.

For TMI, however, our estimated scale of ionicity should give values ranging from 65% to 75%, when we look at the figures of the fractional ionic charge Z calculated for TMH in the framework of a deformation dipole model (see, for instance, Table III of Ref. 34). Quite comparable figures for the net charge Z of the family of TMH may also be found by considering the results of the extended shell model by Benedek and Frey³⁵ as far as the scale of ionicity is concerned (see also Tables I and V of Ref. 35). Furthermore, in a forthcoming paper,³⁶ we plan

to discuss the values of f_i of TMI calculated by using the Phillips³⁷ and Van Vechten theory³⁸ on the ionicity of the chemical bond in crystals. As a matter of fact, we have extended this theory to layered structures of the CdI_2 -type, in the same way it was successfully applied to tin dichalcogenides.³⁹ The calculated Phillips ionicity has given the following values: FeI_2 , 0.76; CoI_2 , 0.75; and NiI_2 , 0.72. Leaving aside for the moment any consideration about the approximation of the model, we feel it, however, necessary to remark that our reported values of f_i for TMI can hardly be directly compared to those of TMC, since the original Pauling's definition of ionicity [see Eq. (2.7) of Ref. 37] was here used³³ without consideration about the number of neighbors in crystals. This fact should alter the ionicity parameter considerably, so that we believe that TMC are less covalent than it would be implied by the reported figures. Apart from this basic difference the series of TMC and TMH present some analogies in the optical properties [see for instance the reflectance spectra of ZrS_2 and ZrSe_2 (Ref. 40)] as far as transition between the valence and conduction band are concerned.

On the basis of the general behavior of the band structure previously presented and by examining the optical data of Sec. III we have been able to reach the following conclusions summarized in Table I.

(1) Γ excitons and interband edges. As in the case of NiCl_2 and NiBr_2 the first strong peak D in TMI (see Fig. 4) is attributed to an exciton associated with the lowest conduction band at Γ_1^+ and the upper valence band at Γ_3^- . The Γ splitting suggest the presence of a second strong exciton from the lower valence band. The spectra of TMI

TABLE I. Energies of the structures in reflectance spectra of TMI at room temperatures. The energy maxima of triplet and doublet excitons and the values of E_g are estimated at low temperatures (20–30 K). The reported theoretical assignments are only valid for NiI_2 and suggested for FeI_2 and CoI_2 , on the ground of similar experimental data. The values listed for NiI_2 have been taken from Ref. 2. NiI_2 has the same crystal structure as NiCl_2 and NiBr_2 , while FeI_2 and CoI_2 have $\text{Cd}(\text{OH})_2$ -type structures. For FeI_2 and CoI_2 , peaks D_1 – D_2 represent spin-orbit splitting and E – I represent critical-point transitions. For NiI_2 , peaks D'_1 – D'_2 represent spin-orbit splitting.

| Label | FeI_2 R or ϵ_2 peaks | Label | CoI_2 R or ϵ_2 peaks | Label | NiI_2 ϵ_2 peaks | Assignments |
|--------|---|--------|---|--------|--------------------------------------|--|
| C | 5.25 | C | 5.23 | C | 5.65 | Triplet exciton |
| D_1 | 5.55 | D_1 | 5.72 | D_1 | 5.82 | Γ exciton |
| D'_1 | 5.95 | D'_1 | 6.20 | D'_1 | 6.25 | $\Gamma_3^-(\frac{3}{2}) \rightarrow \Gamma_1^+$: E_g |
| D_2 | 6.40 | D_2 | 6.45 | D_2 | 6.40 | Γ exciton |
| D'_2 | 6.75 | D'_2 | 6.85 | D'_2 | 7.14 | $\Gamma_3^-(\frac{1}{2}) \rightarrow \Gamma_1^+$ |
| E | 8.00 | | 8.00 | | 8.5 | $Z_3^- \rightarrow Z_1^+$: 7.8 |
| | | E | | E | | $F_2^- \rightarrow F_1^+$: 8.3 |
| F | 9.00 | F | 9.20 | F | 9.20 | $L_2^- \rightarrow L_1^+$: 9.2 |
| | | | | | | $Z_3^+ \rightarrow Z_2^-$: 9.7 |
| G | 10.20 | G | 10.30 | G | 10.00 | $\Gamma_3^+ \rightarrow \Gamma_2^-$: 10.20 |
| | | | | | | $L_2^- \rightarrow L_1^+$: 10.20 |
| H | 14.00 | H | 14.00 | H | 14.00 | $F_2^- \rightarrow F_1^+$: 14.2 |
| | | | | | | $Z_1^+ \rightarrow Z_3^-$: 14.8 |
| I | 15.70 | I | 16.50 | | | $Z_1^+ \rightarrow Z_3^-$: 14.8 |

chlorides, bromides, and iodides show clearly the existence of these pairs of peaks labeled as Γ excitons. The paired peaks D' indicate the onset of the interband transitions, which according to the band structure should be the parent of an M_0 -type reflection edge resulting from a similar joint density of states originating from the valence and conduction bands at Γ . We remark that most of the oscillator strength has gone into the creation of the strong excitons Γ , which make the interband continua weak. The edge corresponding to the upper valence band due to $\Gamma_3^+ \rightarrow \Gamma_2^-$ transitions is clearly visible in all iodides (peak G).

(ii) *Z interband edge* [substitute A for Z in the following in case of $\text{Cd}(\text{OH})_2$ -type structure]. According to the band structure the three degenerate valence bands and the lowest conduction band at Z_1^+ give a joint density of states characterized by a strong curvature and a singularity of type M_1 or M_2 . No exciton peaks have been detected at this point which would give an hyperbolic exciton. Transitions $Z_3^- \rightarrow Z_1^+$ origin the peaks E and $Z_1^+ \rightarrow Z_3^-$ give the peak M .

(iii) *Higher-energy transitions*. At energies higher than those corresponding to transitions to Γ_1^+ , we see the presence of a high density of states, which corresponds to conduction branches L_1^+ , F_1^+ , and Z_1^+ in the CdCl_2 -type structure nomenclature. For energies higher than 10 eV the interpretation of the spectra is difficult since several electronic transitions are possible and at the same time the spectra show broad structures. Finally, above 15–16 eV the one-electron transitions from the valence band are practically exhausted and plasma oscillations of the valence electrons are present in the crystal.

One more point deserves attention in connection with the self-consistent band structure of TMH (and TMI) determined by the intersecting-sphere model.^{14,15} This model is expected to provide accurate results not only for the valence-band region but also for the low-lying conduction levels. One of the reasons for considering with confidence the band structures of TMH, on which all the present assignments are based, is to be found in the results of band calculations recently made on MgCl_2 ,¹² where the tight-binding method was used in the calculation of the band structure of core- and valence-band states and the orthogonal plane-wave method using the empty lattice model was considered to determine the conduction-band structure. These band calculations were found to agree very closely to the results obtained on MgCl_2 (same band structure as NiCl_2 and NiBr_2) by the model employed by Antoci and Mihich. We will discuss the fine structure in the region of the Γ excitons, occurring in the TMI in the energy region 5–6 eV, which we have already commented upon previously.^{1,2} Similar excitons observed in cubic alkali halides, have been discussed in the Onodera-Toyozawa theory. The observation in the alkali halides that the ratio of the absorption intensities of the $(\frac{3}{2}, \frac{1}{2})$ and $(\frac{1}{2}, \frac{1}{2})$ excitons is often appreciably smaller than 2:1, as expected for the simplest model, is explained in this theory by considering the electron-hole exchange interaction which mixes the two exciton states and causes changes of the intensity ratio. The intensity ratio and the

splitting of the exciton doublet in this theory is determined by this exchange interaction Δ and by the spin-orbit splitting of the upper valence band λ . The observed spectra (Fig. 4) for the Γ excitons in FeI_2 , CoI_2 , and NiI_2 at 300 K show two broad peaks with a splitting of approximately 0.7 eV and an intensity ratio of approximately 1:2 for all three TMI. In NiI_2 these observations were explained in terms of the OT theory, with the parameters $\Delta=0.43$ eV and $\lambda=0.60$ eV.² The value of λ corresponds quite well to the spin-orbit splitting constant $\lambda_0=0.68$ eV for $5p$ electrons of the free iodine ion. In view of the similarities in the spectra of the three TMI we suggest that this interpretation is also valid for CoI_2 and FeI_2 , with the same values of λ and Δ . Indeed one expects approximately the same values for λ and Δ because these parameters refer to the valence and conduction bands which are essentially the same in the three TMI. At lower temperatures (30 K, see Fig. 4) the Γ exciton region shows fine structure with several sharp peaks. In NiI_2 one of these peaks C was assigned to the triplet exciton, and its position with respect to the other exciton peaks could be explained quite well with the OT theory, using the parameters mentioned above.²

A similar explanation in terms of the OT theory of the sharp peaks in the spectra of CoI_2 and FeI_2 was attempted but was not successful. We suggest that this is due to the effect of the exchange interaction of the electron of the exciton (in conduction band $4s$ -like states) with the localized magnetic moment of the $3d$ electrons of the metal. Such an exchange interaction will produce a splitting of the exciton levels, and a mixing of the unperturbed singlet and triplet exciton states, which complicate the low-temperature assignments for the exciton structures and the intrinsic absorption edge. A consequence of this mixing is also a transfer of transition intensity to (perturbed) tripletlike exciton states. One expects that this exchange interaction increases in the series NiI_2 - CoI_2 - FeI_2 , as a consequence of the increasing spin of the $3d$ shell ($S=1, \frac{1}{2}, 2$, respectively). This explains that the simple OT theory, which does not take account of the exchange interaction with the $3d$ electron spin, may explain the spectra of NiI_2 rather well, but is not sufficient to interpret the spectra of CoI_2 and FeI_2 . It also explains why splitting and intensities of the peaks are different for the three TMI at low temperature. At high temperature the peaks are broadened, the fine structure disappears, and only the splitting due to the spin-orbit coupling in the valence band is observed (peaks D in Fig. 4).

V. CONCLUSIONS

The analysis of the ultraviolet properties of crystals of TMI, here investigated for the first time, and attempted on the basis of available band-structure calculations, has yielded a satisfactory description of low-lying excited states. Excitonic structures derived from the Γ point in the Brillouin zone are responsible for the dominant structures in the optical spectra in the low-energy region. The energies of the plasma peaks associated with excitation of the valence electron gas have been found around 15–16 eV in good agreement with the calculated values.

The width of the energy-loss peaks are indicative of

some overlap between electronic band-band and plasmon excitations which favors the damping of plasma waves in crystals via the linear electron-plasmon interaction. The values of the forbidden $p \rightarrow s$ gaps and high-frequency dielectric constants $\epsilon_{\infty}^{xx} \simeq \epsilon_{\text{eff}}(E)$, are also reported for TMI. Peaks C are attributed to triplet excitons in terms of the Onodera-Toyozawa theory. The splitting is assumed to arise from exchange interaction of the electron spin of the exciton in the $4s$ -like state with the spin of the $3d$ electrons. In order to assign the observed peaks in the Γ exciton region, an extended theory of exciton which takes into account the spin-orbit coupling in the valence band, the exchange interaction between electron and hole and the exchange interaction of electron (and hole) with localized $3d$ spins is needed.

ACKNOWLEDGMENTS

The authors thank the technical staff of the Laboratoire de l'Accélérateur Linéaire for providing the ultraviolet beam during the experimental course. They also wish to thank Professor C. Haas for his suggestion about extending the Onodera-Toyozawa theory to include materials with magnetic properties. One of us (I.P.) gratefully acknowledges the Centre National de la Recherche Scientifique (CNRS) for financial support during his stay at the Université de Paris-Sud. The investigation was supported in part by the Netherlands Foundation for Chemical research (SON) with financial aid from the Netherlands Organization for Advancement of Pure Research (ZWO).

- ¹I. Pollini, J. Thomas, G. Jézéquel, J. C. Lemonnier, and R. Mamy, *Phys. Rev. B* **27**, 1303 (1983).
- ²I. Pollini, J. Thomas, G. Jézéquel, J. C. Lemonnier, and A. LenseLink, *Phys. Rev. B* **29**, 4716 (1984).
- ³I. Pollini, J. Thomas, A. LenseLink, and J. C. Lemonnier, *Annals of the Israel Physical Society* (Hilger, Bristol, 1983) and *Isr. Phys. Soc. Jerusalem* **6**, 255 (1983).
- ⁴Y. Onodera and Y. Toyozawa, *J. Phys. Soc. Jpn.* **22**, 833 (1967).
- ⁵H. Fesefeldt, *Z. Phys.* **64**, 741 (1930).
- ⁶M. R. Tubbs, *J. Phys. Chem. Solids* **29**, 1191 (1968).
- ⁷R. W. G. Wyckoff, *Crystal Structures* (Interscience, New York, 1963), Vol. 1.
- ⁸W. van Erk, thesis, University of Groningen (1974).
- ⁹L. G. van Uitert, H. J. Williams, R. C. Sherwood, and J. J. Rubin, *J. Appl. Phys.* **36**, 1029 (1965).
- ¹⁰H. Bizette, C. Terrier, and B. Tsai, *C. R. Acad. Sci.* **246**, 250 (1958).
- ¹¹J. B. Goodenough, *Magnetism and the Chemical Bond* (Interscience, New York, 1963).
- ¹²S. Kinno and R. Onaka, *J. Phys. Soc. Jpn.* **49**, 1379 (1980).
- ¹³S. Kinno and R. Onaka, *J. Phys. Soc. Jpn.* **50**, 2073 (1981).
- ¹⁴S. Antoci and L. Mihich, *Solid State Commun.* **31**, 861 (1979).
- ¹⁵S. Antoci and L. Mihich, *Phys. Rev. B* **18**, 5768 (1978); **21**, 3383 (1980).
- ¹⁶V. V. Pechkovskii and A. V. Sofronova, *Russ. J. Inorg. Chem.* **11**, 838 (1960).
- ¹⁷W. E. Zaugg and N. W. Gregory, *J. Phys. Chem.* **70**, 486 (1966).
- ¹⁸S. R. Kuindersma, *Phys. Status Solidi B* **107**, K163 (1981); thesis, University of Groningen (1980).
- ¹⁹C. Kittel, *Quantum Theory of Solids* (Wiley, New York, 1963), Chap. 6.
- ²⁰D. Pines, *Rev. Mod. Phys.* **28**, 184 (1956).
- ²¹L. Marton, *Rev. Mod. Phys.* **28**, 172 (1956).
- ²²L. Van Hove, *Phys. Rev.* **95**, 249 (1954).
- ²³P. Nozières and D. Pines, *Phys. Rev.* **113**, 1254 (1959).
- ²⁴S. L. Adler, *Phys. Rev.* **126**, 413 (1962).
- ²⁵H. Eherenreich and M. H. Cohen, *Phys. Rev.* **115**, 786 (1959).
- ²⁶C. Horie, *Prog. Theor. Phys.* **21**, 113 (1959).
- ²⁷I. Pollini, G. Benedek, and J. Thomas, *Phys. Rev. B* **29**, 3617 (1984).
- ²⁸It must be recalled that the condition for the existence of plasma oscillation at frequency ω is just $\hat{\epsilon}(\omega)=0$. The general solution is given by a complex frequency $\omega=\Omega_p-i/\tau$, where the relaxation time describes the damping of the plasma wave. See also Refs. 29 and 30.
- ²⁹P. Wolff, *Phys. Rev.* **92**, 18 (1953).
- ³⁰H. Kanezawa, *Prog. Theor. Phys.* **13**, 227 (1955).
- ³¹R. B. Murray, R. A. Bromley, and A. D. Yoffe, *J. Phys. C* **5**, 746 (1972).
- ³²L. F. Mattheis, *Phys. Rev. B* **8**, 3719 (1973).
- ³³F. R. Gamble, *J. Solid State Chem.* **9**, 358 (1974).
- ³⁴I. Pollini, G. Spinolo, and G. Benedek, *Phys. Rev. B* **22**, 6369 (1980).
- ³⁵G. Benedek and A. Frey, *Phys. Rev. B* **21**, 2482 (1980). Here we find, for example, the value of $Z=0.75$ for VI₂.
- ³⁶I. Pollini and J. Thomas (unpublished).
- ³⁷J. C. Phillips, *Rev. Mod. Phys.* **42**, 317 (1970), and references quoted therein.
- ³⁸J. A. Van Vechten, *Phys. Rev.* **182**, 891 (1969).
- ³⁹V. P. Gupta, P. Agarwal, A. Gupta, and V. K. Srivastava, *J. Phys. Chem. Solids* **43**, 291 (1982).
- ⁴⁰D. L. Greenaway and R. Nitsche, *J. Phys. Chem. Solids* **26**, 1445 (1965).